Journal of Marine Research, 58, 895–917, 2000

The role of eddies in the isopycnic transfer of nutrients and their impact on biological production

by Mei-Man Lee[1] **and Richard G. Williams**[2]

ABSTRACT

Eddies provide a systematic, large-scale transfer of tracers and nutrients along isopycnals through a combination of eddy-induced diffusion and advection. The nutrient distribution is controlled by advection, rather than diffusion, when the nutrient lifetime exceeds a timescale given by κ/V^2 where κ is the lateral diffusivity and V is the characteristic transport velocity. Idealized, eddy-resolving experiments are conducted using an isopycnic model configured for a zonal channel. Whether the eddies act to enhance or inhibit biological production depends on the location of the nutrient source and the nutrient lifetime. For a subtropical gyre and the Southern Ocean, the eddy-induced diffusion and advection are likely to oppose each other over the euphotic zone but reinforce each other at depth. Over the euphotic zone, the combination of eddy diffusion and Ekman advection of nutrients should dominate the opposing eddy-induced advection. This lateral transfer becomes more important for long-lived nutrients, such as dissolved organic nitrogen, within the euphotic zone.

1. Introduction

Enhanced levels of biological production have been attributed to the action of mesoscale eddies and fronts in observational studies (e.g., Strass, 1992; Denman and Abbott, 1994) and numerical high-resolution experiments (e.g., Levy *et al.*, 1998; Oschlies and Garcon, 1998; Mahadevan and Archer, 2000). The exact mechanism by which eddies enhance biological production is less clear. Recent studies have emphasized the *local* response to the eddy circulation. Eddies may lead to an enhancement in production through a rectified upwelling of nutrients (McGillicuddy and Robinson, 1997). In addition, the eddy transfer of heat may lead to a shallowing of the mixed layer, which in turn can lead to an earlier onset of the spring bloom through biota experiencing more light (Levy *et al.*, 1998). In our study, we focus on the larger-scale response of eddies and how they can systematically transfer nutrients along isopycnals. This eddy transfer of nutrients might be particularly important across frontal zones, such as in the Southern Ocean, and in sustaining export production over the flanks of the subtropical gyres.

Eddies transfer tracers along isopycnals through a rectified advection, as well as a down-gradient diffusion. The eddy diffusion fluxes tracer down-gradient (Fig. 1a,b),

1. Southampton Oceanography Centre, Empress Dock, Southampton, SO14 3ZH, United Kingdom.
2. Corresponding author: Oceanography Laboratories, Department of Earth Sciences, University of Liverpool, Liverpool, L69 7ZL, United Kingdom. ***email: ric@liv.ac.uk***

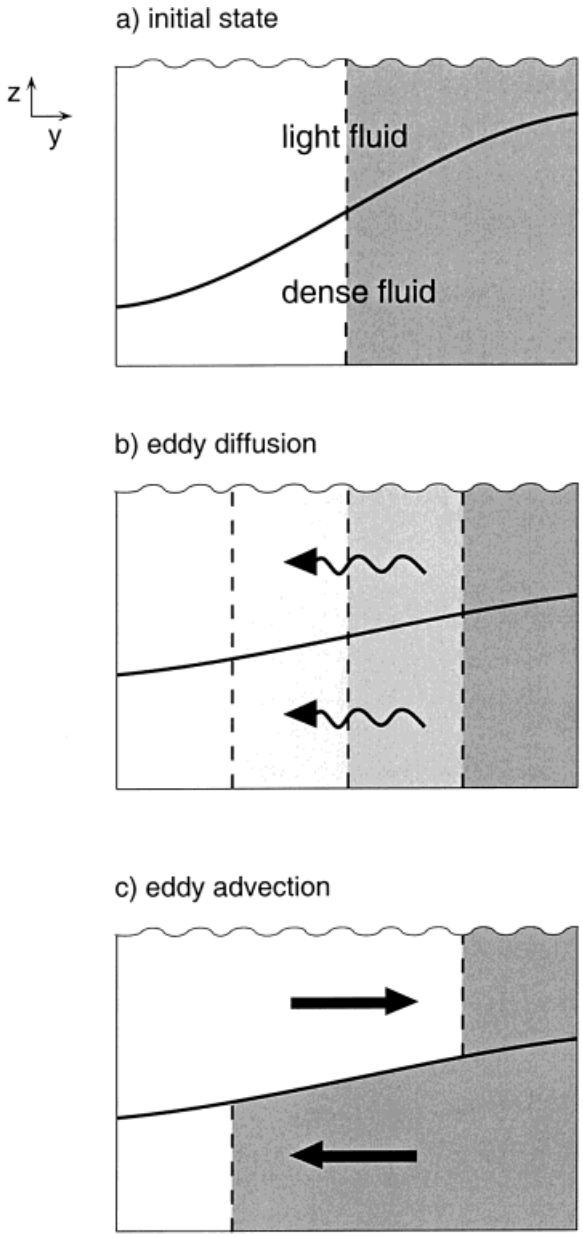

Figure 1. Schematic of eddy transfer of tracer. Eddies are generated through the slumping of the interface between light and dense fluid. In this thought experiment, an initial tracer contrast in (a) is modified through an eddy-induced diffusion in (b) and advection in (c). The eddy-induced advection arises from the slumping of the interface. This diffusion and advection can oppose or reinforce each other in spreading tracer, as illustrated in the upper and lower layers, respectively.

eventually leading to a uniform distribution if there are no external sources. The eddy advection depicted in Figure 1c is a secondary circulation arising through the slumping of isopycnals, which is associated with a correlation in the velocity and vertical spacing between isopycnals (Rhines, 1982; Gent *et al.,* 1995). The advective transfer can be up- or down-gradient, and so can oppose or reinforce the diffusive transfer according to the tracer source distributions (Fig. 1c). The advective and diffusive transfer of tracers is illustrated in eddy-resolving experiments by Lee *et al.* (1997); referred to as LMW henceforth. The importance of the eddy transfer also depends on the relative magnitude of the time-mean advection. Over the euphotic zone, the wind-driven Ekman flow is particularly important, since the horizontal Ekman flux often has a large component directed across nutrient contours (Williams and Follows, 1998).

In this study, we explore how the eddy diffusion and advection influence nutrients with different lifetimes in the euphotic zone. Simplified eddy-resolving experiments are conducted at the sub-basin scale intermediate between that of an individual eddy (Levy *et al.,* 1998) and an entire basin (Oschlies and Garcon, 1998). Our experiments focus on (i) how eddies transfer nutrients into the euphotic zone through advection or diffusion along isopycnal layers, (ii) how the dominant eddy transfer mechanism varies according to the lifetime of the nutrients, and (iii) how the total transport including the wind-driven Ekman and eddy transfer controls the response in realistic regimes.

In Section 2, the relative importance of eddy advection and diffusion is discussed theoretically for tracers with different lifetimes. In Section 3, idealized eddy-resolving experiments are conducted examining how tracers are transferred across a baroclinically, unstable jet within a zonal channel. The experiments include buoyancy forcing to maintain the jet, as well as cases with and without wind forcing. In Section 4, the idealized experiments are modified to include nitrate and dissolved organic nitrogen (DON), which have short and long lifetimes in the euphotic zone, respectively. In Section 5, the results are discussed in terms of how eddies might play a role in transferring nutrients across the flanks of oligotrophic, subtropical gyres and zonal currents, such as the Antarctic Circumpolar Current.

2. Eddy-induced transport and diffusion

Tracer distributions are controlled by the location of sources and sinks, and the action of the circulation and mixing in transferring the tracer. The tracer evolution is given by

$$\frac{\partial N}{\partial t} + \mathbf{u} \cdot \nabla N = S, \tag{1}$$

where N is an idealized tracer or nutrient, $\mathbf{u}$ is the velocity and S is a tracer source. Following Gent *et al.* (1995), applying a zonal average and a time average over a density layer, the time-averaged tracer concentration evolves through advection, eddy diffusion

and the source (second to fourth terms, respectively):

$$\frac{\partial \overline{N}}{\partial t} + \overline{V}\frac{\partial \overline{N}}{\partial y} = \frac{1}{\overline{h}}\frac{\partial}{\partial y}\left(\overline{h}\kappa\frac{\partial \overline{N}}{\partial y}\right) + \overline{S}, \tag{2}$$

where the overbar represents a zonal average over the domain and a time average extending over many eddy lifetimes. The tracer is advected by the transport velocity, $\overline{V}$, which is the sum of the Eulerian time-mean velocity, $\overline{v}$, and an eddy-induced rectified velocity or 'bolus' velocity, v^*,

$$\overline{V} = \overline{v} + v^*,$$

where $v^* = \overline{v'h'}/\overline{h}$ depends on the correlations in velocity and layer thickness, h, and a prime represents a deviation from the zonal and time average. The bolus velocity is particularly large in regions of baroclinic instability where isopycnals slump and v' and h' are positively correlated.

The tracer is diffused by the time-varying flow with the eddy-induced diffusivity, κ, defined by the eddy flux closure, $\overline{(hv)'N'} = -\kappa\overline{h}\partial\overline{N}/\partial y$.

a. Tracer spreading without interior sources or sinks

Following LMW, consider how eddies control the spreading of a point source of tracer either by advection or diffusion in the limit of no source or sink. If there is a balance between temporal change and advection in (2), then scale analysis suggests that the tracer spreads over a meridional scale given by

$$L_{\text{adv}} \sim \overline{V}t, \tag{3}$$

where t is time and $\overline{V}$ is the transport velocity. Alternatively, if diffusion dominates the tracer evolution, then scale analysis of (2) suggests that the tracer spreads over a meridional scale given by

$$L_{\text{dif}} \sim (\kappa t)^{1/2}. \tag{4}$$

The ratio of these length scales is given by

$$\left(\frac{L_{\text{adv}}}{L_{\text{dif}}}\right)^2 \sim \frac{\overline{V}^2}{\kappa}t.$$

Thus, for given nonzero κ and $\overline{V}$, the initial spreading will be diffusive, since the ratio of $L_{\text{adv}}/L_{\text{dif}}$ is small. Over longer timescales, however, advection becomes important, as the horizontal scales inflate and may eventually dominate over diffusion.

b. Tracer spreading with a surface sink

Now consider how the tracer spreading alters through the inclusion of a surface sink depicted simply by $S = -\alpha N$ where α is an inverse timescale. For a point release of tracer,

the tracer spreads meridionally with the advective and diffusive scales inflating until the surface sink becomes important. Hence, the advective and diffusive scales in (3) and (4) reach limiting values of

$$L_{\mathrm{adv}} \sim \overline{V}\alpha^{-1},$$

$$L_{\mathrm{dif}} \sim (\kappa\alpha^{-1})^{1/2},$$

and the ratio is

$$\left(\frac{L_{\mathrm{adv}}}{L_{\mathrm{dif}}}\right)^2 \sim \frac{\overline{V}^2}{\kappa\alpha}. \tag{5}$$

These limiting horizontal scales, L_{adv} and L_{dif}, become comparable when the nutrient lifetime α^{-1} is a similar magnitude to a dynamical timescale given by $\kappa/\overline{V}^2$ from (5), which is 4 months for $\overline{V} \sim 1$ cm s^{-1} and $\kappa \sim 1000$ m^2 s^{-1}. The tracer can be defined as either long- or short-lived according to whether its lifetime is greater or shorter than this dynamical timescale, $\kappa/\overline{V}^2$. The final equilibrium state for long- or short-lived tracers should be controlled by advection or diffusion, respectively.

Within the euphotic zone, the lifetime of a nutrient is limited through biological consumption. In nutrient-limited regions, nitrate has a lifetime of typically 1 month or less in the euphotic zone, whereas semi-labile, dissolved organic nitrogen (DON) has a longer lifetime of several months to a year. Consequently, we expect that nitrate is a short-lived tracer, transferred by diffusion, whereas DON might be a long-lived tracer, transferred by the transport velocity. Note that these lifetimes become much longer whenever any other processes are limiting biological consumption, such as zooplankton grazing, solar irradience or the supply of trace metals.

In the following eddy-resolving experiments, we examine the evolution of short- and long-lived idealized tracers in Section 3, as well as for nitrate and DON in Section 4.

3. Model tracer experiments

a. Model configuration

The eddy transfer of nutrients is examined using an isopycnic model (Bleck and Smith, 1990) configured for an idealized, re-entrant, zonal channel (Fig. 2); it is a modified version of that used in LMW. Eddies are explicitly resolved with a model horizontal resolution of 10 km, whereas there is a larger Rossby radius of deformation of 60 km. The channel extends 1000 km meridionally and 600 km zonally, and is 1000 m in depth. There are five isopycnic layers with potential densities of $\sigma = 25.2$, 25.8, 26.4, 27.0 and 27.6 kg m^{-3}, and an explicit mixed layer is not included. In order to focus on the role of the eddy transfer, we avoid the issue of convective mixing which is important for seasonal and interannual changes in nitrate supply (Williams *et al.*, 2000).

Buoyancy forcing is incorporated in buffer zones (50 km wide) along the southern and northern walls, which leads to a poleward shoaling of the layer interfaces in the interior

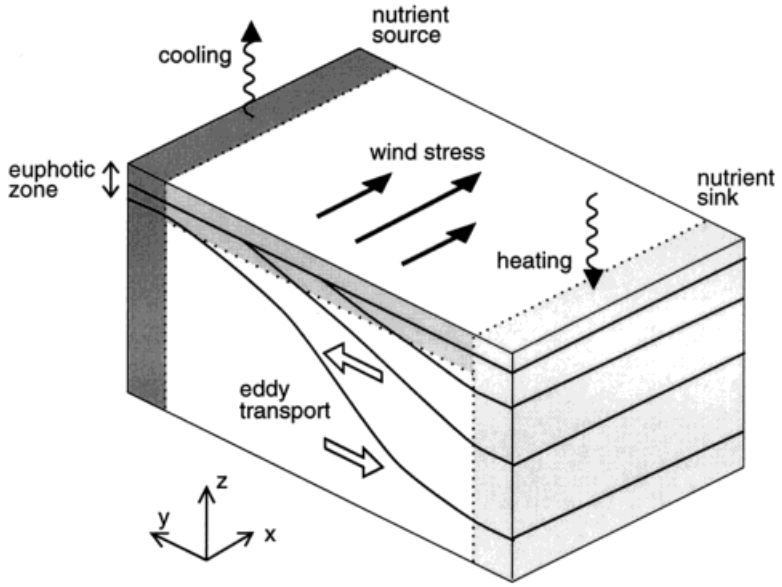

Figure 2. Schematic of model domain consisting of a zonally-periodic channel with five density layers which are forced by heating and cooling in relaxation zones on the southern and northern boundaries. Idealized tracers and nutrient sources are included in the northern or southern boundaries. The tracers are transferred meridionally through the eddy-induced transport and diffusion. In later experiments, a surface wind stress is included which provides an additional Ekman-driven circulation.

(Fig. 3, dotted lines). The buoyancy forcing from the buffer zones creates a time-mean zonal jet with typical velocities of 20 cm s^{-1}. A surface buoyancy relaxation is also included in order to maintain the meridional temperature gradient over the upper 100 m; the relaxation time scale of the buoyancy forcing is 2 hours. Wind forcing is included in later integrations in Sections 3e and 4, where the Ekman stress is applied over a surface thin layer, which is artificially forced to have a constant thickness and density.

b. Eddy-induced circulation

The zonal jet is baroclinically unstable and generates a vigorous eddy field. The slumping of layer interfaces generates a secondary circulation with a poleward surface flow and an equatorward bottom flow—in accord with the eddy transport depicted in Figure 1c. The eddy-driven transport or 'bolus' velocity, v^*, reaches 1 cm s^{-1} over the upper layers and -0.3 cm s^{-1} over the bottom layer. In comparison, there is no significant time-mean meridional velocity, $\bar{v}$, with no wind forcing. Consequently, the transport velocity, $\overline{V} = \bar{v} + v^*$, is directed poleward in the upper layers and equatorward in the bottom layer (Fig. 3).

The transport is isopycnic in the interior, but crosses the isopycnic interfaces where there is buoyancy forcing over the upper 100 m and in the northern and southern boundary zones.

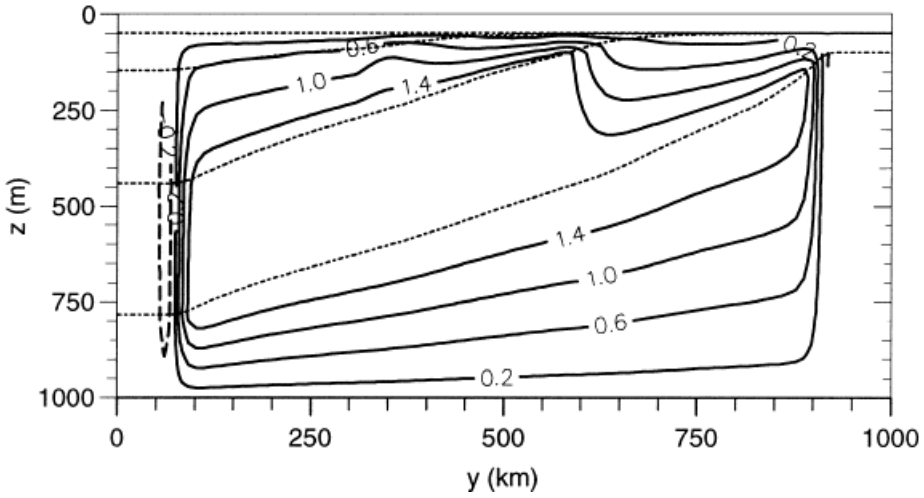

Figure 3. Meridional section showing a streamfunction ($m^2\ s^{-1}$) for the transport velocity, $\overline{V} = \bar{v} + v^*$, where $\bar{v}$ is the time-mean Eulerian velocity and v^* is the eddy-induced transport or bolus velocity. For this buoyancy-forced integration, the transport velocity is dominated by the eddy-induced contribution. The temporal and zonal average of layer interfaces are marked by the dotted lines.

c. Idealized tracer solutions

The idealized tracer concentration, N, is integrated online using the tracer equation

$$\frac{\partial N}{\partial t} + \mathbf{u} \cdot \nabla N = -\alpha N + \frac{\kappa_n}{h} \nabla \cdot (h \nabla N), \tag{6}$$

where $\mathbf{u}$ is the horizontal velocity, α is the inverse decay time scale, and κ_n is the explicit numerical diffusivity. This explicit diffusivity is only included to diffuse tracer variance accumulating on the grid cell and has a relatively small value of 50 $m^2\ s^{-1}$.

Idealized tracer sources are included on the northern and southern boundaries with source values of either 1 or 0. In addition, the tracer lifetime is limited over the upper 100 m, which may be viewed as the euphotic zone, by a surface sink depicted by $-\alpha N$. The tracer equation is integrated for 8 years with the tracer having an initial concentration of 0.

The tracer spreading is controlled by the tracer source and the direction of the transport velocity (as shown by the streamfunction in Fig. 3). Instantaneous tracer snapshots reveal the eddy activity, but the meridional spreading of tracer is asymmetrical and depends on where the tracer is released (Fig. 4).

For a southern source, the tracer spreads systematically poleward at the surface (Fig. 4a). This spreading is achieved through a combination of the eddy-induced diffusion and advection; note that there is no significant time-mean meridional velocity in this integration. The tracer spreads in a similar manner over the upper four layers, but is relatively confined in the bottom layer (Fig. 5a). This variation is consistent with the slumping of

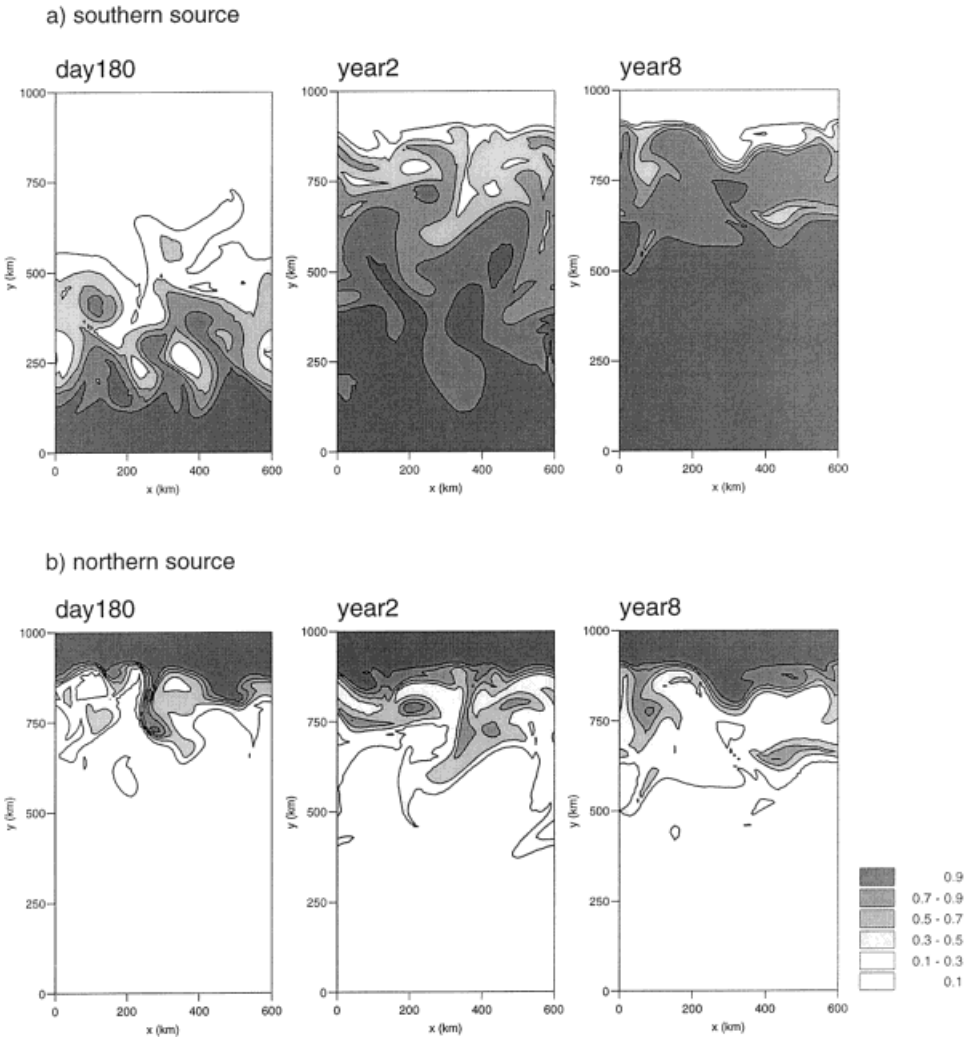

Figure 4. Instantaneous maps of the tracer distribution at day 180, years 2 and 8 in the upper 100 m for a tracer source on either (a) southern or (b) northern boundary. The asymmetrical spreading of tracer in (a) and (b) is due to the poleward transport velocity in the surface layer.

isopycnals driving a polewards flow over the upper four layers and a return equatorward flow in the bottom layer (Fig. 3); note that the slumping is arrested through the inclusion of the buoyancy forcing in the northern and southern buffer zones.

For a northern source, there is no significant tracer spreading at the surface, despite the evident eddy activity (Fig. 4b). The other upper layers likewise have low tracer concentrations and the only significant tracer spreading is confined to the bottom layer (Fig. 5b). This response is due to the eddy-induced advection and diffusion opposing each other over the upper four layers, but reinforcing each other over the bottom layer.

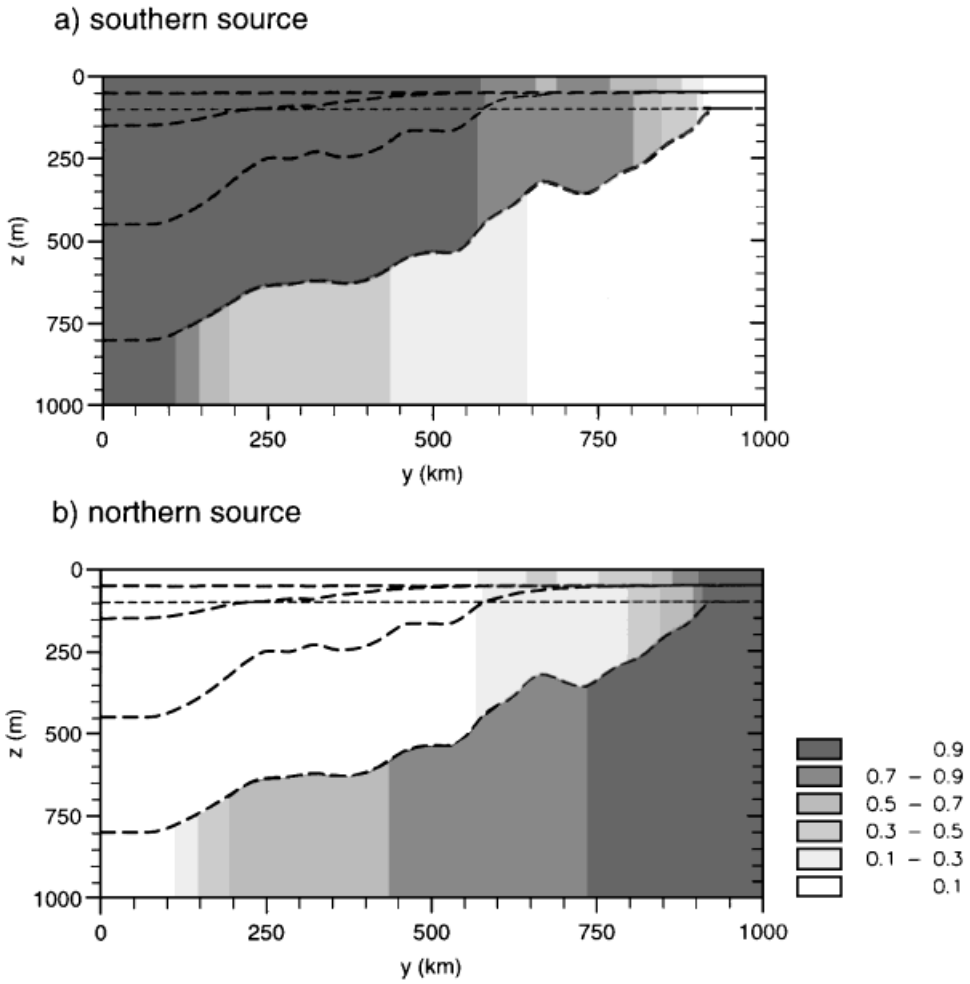

Figure 5. Meridional tracer sections for (a) southern and (b) northern sources after 8 years with only buoyancy forcing applied; a tracer sink is included on the opposing boundary. The enhanced poleward spreading of tracer in the upper layers and equatorward spreading in the bottom layer is due to the transport streamfunction shown in Figure 3.

The surface tracer concentrations reduce according to their lifetime over the upper 100 m. For the southern source, the meridional scale of tracer spreading becomes smaller (Fig. 6a), but there is no significant change for the northern source, since little tracer escapes into the interior (Fig. 6b).

d. Diagnostics of the advection and diffusive flux

The relative importance of the eddy-induced advection and diffusion is revealed by diagnosing the time-averaged and zonally-averaged flux form of the tracer equation (Gent

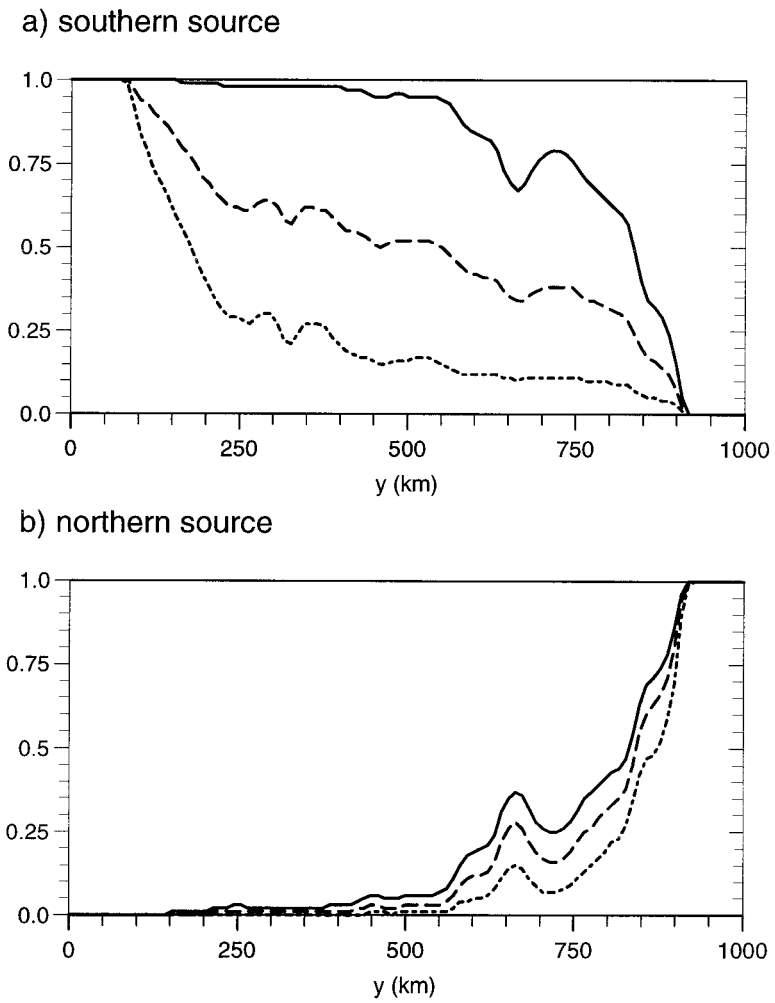

Figure 6. Meridional tracer variation in the surface layer for (a) southern or (b) northern sources after 8 years with only buoyancy forcing applied. The tracer is either conserved in the interior (full line) or has a surface lifetime of 1 year (long dashed line) or 3 months (short dashed line).

et al., 1995):

$$\frac{\partial}{\partial t}(\overline{hN}) + \frac{\partial}{\partial y}(\overline{hv})\overline{N} = -\frac{\partial}{\partial y}\overline{(hv)'N'} - \alpha\overline{hN}. \tag{7}$$

The total tracer flux, $\overline{hvN}$, is separated into the advective flux, $\overline{hv}\,\overline{N}$, and the diffusive flux, $\overline{(hv)'N'}$, where the overbar is the zonal and time average evaluated over the last 4 years of tracer integration, and the prime is the deviation from this average.

Firstly, consider the case with a southern source. For the upper four layers, the advective

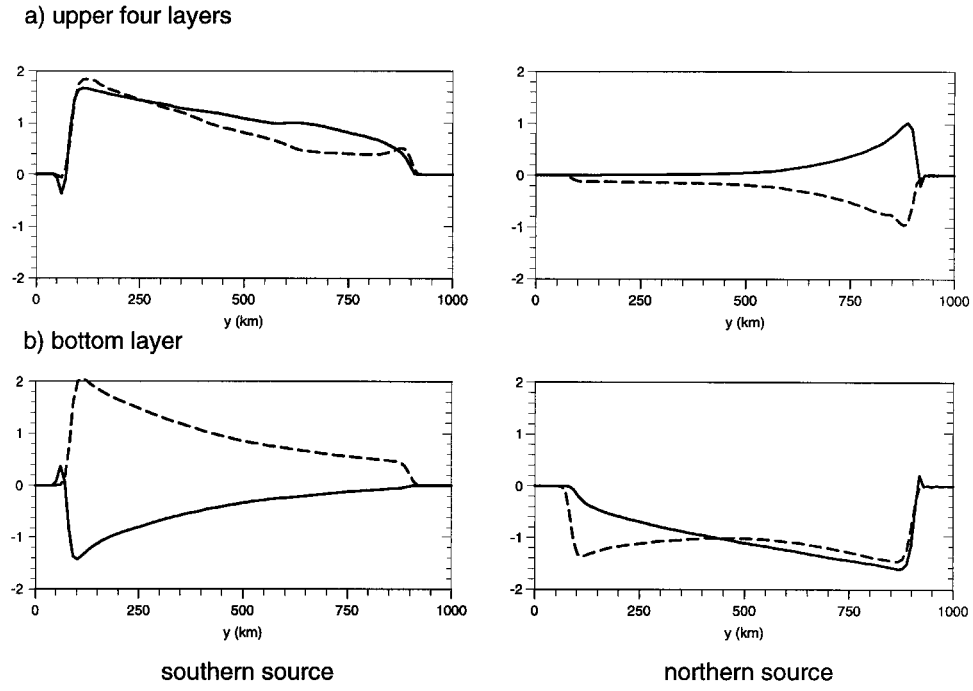

Figure 7. The meridional tracer fluxes for a southern source (left panel) or northern source (right panel). The advective flux, $\overline{vh}\,\overline{N}$, and the diffusive flux, $\overline{(vh)'N'}$, are depicted by the solid and dashed lines, respectively. The tracer lifetime in the surface layer is 1 year. The fluxes are shown either averaged over (a) the upper four layers or (b) the bottom layer.

and diffusive fluxes both act to transfer tracer poleward. The diffusive and advective fluxes are comparable in magnitude for a long-lived tracer with a lifetime of 1 year (Fig. 7a). The diffusive flux becomes larger for a tracer with a shorter lifetime of 3 months (not shown). In the bottom layer, the advective flux opposes the diffusive flux, which inhibits any poleward spreading of tracer (Fig. 7b).

Secondly, for a northern source, the reverse situation occurs. The advective and diffusive fluxes oppose each other over the upper four layers (Fig. 7a): the advective and diffusive fluxes are comparable in magnitude near the northern boundary, but the down-gradient diffusive flux dominates in the interior. The advective and diffusive fluxes reinforce each other over the bottom layer and have a similar magnitude (Fig. 7b).

Therefore, the diffusive flux is always acting to spread the tracer away from the source. However, the effectiveness of the diffusion is limited by the advection. There is rapid spreading of the tracer when the diffusion and advection reinforce each other, but a reduced influx of tracer when the diffusion and advection oppose each other.

We now consider how these results are modified by incorporating wind forcing and examine the competition between the Ekman and eddy-induced circulation.

e. Incorporating wind forcing

The zonal channel is now forced with an eastward wind-stress, varying meridionally as $\tau_o \sin(\pi y/L)$, together with the previous form of buoyancy forcing; where $\tau_o = 0.1$ N m^{-2} and L is the north-south extent of the basin. The stress drives a time-mean, meridional velocity, $\bar{v}$, consisting of an equatorward, surface Ekman flux and a poleward return flow in the bottom layer (Fig. 8a). This time-mean Eulerian circulation opposes the eddy-induced overturning circulation (Fig. 8b). This competition is due to the wind forcing acting to steepen isopycnals and increase available potential energy, whereas the eddy transport is attempting to flatten isopycnals and release available potential energy. The resulting transport velocity, $\overline{V} = \bar{v} + v^*$, can have either sign depending on the relative magnitude of the time-mean Eulerian and eddy-induced contributions. In our particular case, the Ekman flux dominates over the upper 100 m, whereas the eddy-induced transport dominates below. The transport velocity is equatorward (-1.4 cm s^{-1}) over the surface layer, poleward over the intermediate layers and equatorward again in the bottom layer (Fig. 8c).

The tracer experiment with a northern source of 1 (and a southern source of 0) is now repeated with the wind forcing included. The tracer now spreads southward from the northern source over the surface layer (Fig. 9). The tracer spreading is in accord with the new transport velocity (Fig. 8c) and down-gradient eddy diffusion. Hence, the Ekman transfer and eddy-induced diffusion dominate, over the opposing eddy-induced advection.

The enhanced tracer spreading induced by the Ekman flow is also revealed in the surface concentration plots in Figure 10 (compared with the nonwind case in Fig. 6b). Incorporating tracers with different surface lifetimes leads to the expected reduction in the meridional scale as the lifetime becomes smaller. We now extend these experiments to examine the eddy transfer of nitrate and DON incorporating recycling of nutrients and more plausible boundary conditions.

4. Coupled nitrate and DON experiments

A coupled nitrate and DON problem is considered, where the nitrate is chosen to be short lived and the semi-labile DON to be long lived in the euphotic zone. Consequently, the meridional scale of the nutrient spreading is likely to be controlled by diffusion for nitrate, but by advection for DON. Thus, DON potentially provides a different nutrient pathway and might enable biological production to occur in nitrate-depleted, oligotrophic surface waters (e.g., Jackson and Williams, 1985), as well as perhaps compensating for the diagnosed divergence in the nitrate flux over the subtropical gyre in the North Atlantic (Rintoul and Wunsch, 1991).

The appropriate lifetime of semi-labile DON is unclear. Model estimates range from several months in the surface to years in the main thermocline (Archer *et al.,* 1997; Yamanaka and Tajika, 1997; Anderson and Williams, 1999). In our study, we choose a lifetime of DON of 1 year, since our study does not include a seasonal cycle in light or mixing. Including the seasonal cycle can act to lengthen the effective lifetime of nutrients

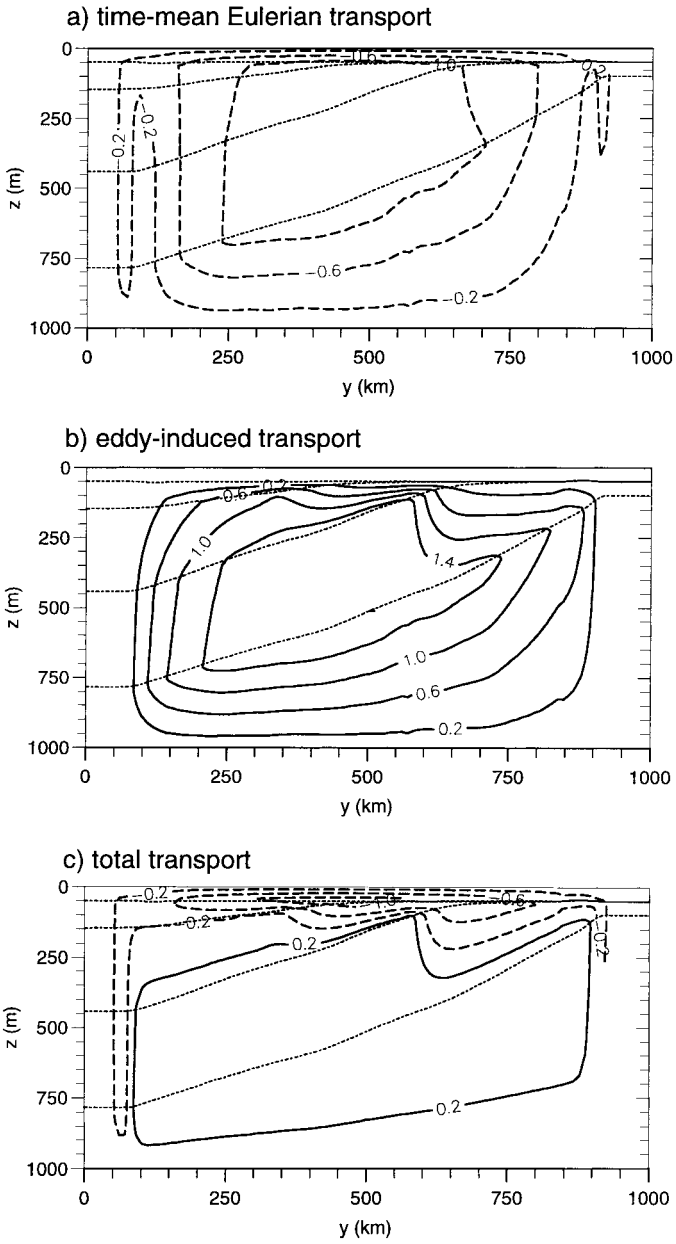

Figure 8. Overturning streamfunctions ($m^2\ s^{-1}$) when wind forcing is included for (a) the time-mean Eulerian velocity, $\bar{v}$, (b) the eddy-induced transport or bolus velocity, v^*, (c) the total transport velocity, $\overline{V} = \bar{v} + v^*$.

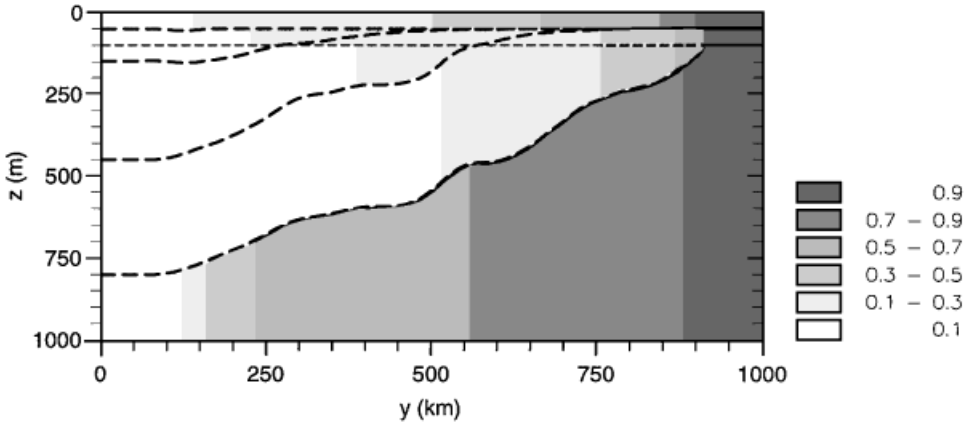

Figure 9. Meridional tracer section with wind forcing after 8 years including a northern source and no surface sink, apart from on the southern boundary.

in the upper ocean through light limitation inhibiting biological consumption during winter.

a. Coupled nutrient model

A simplified coupled nitrate and DON model is employed, which includes a different cycling of nitrate and DON; see Najjar *et al.* (1992) for a more sophisticated version. For simplicity, we ignore the seasonal cycle in light intensity and convection.

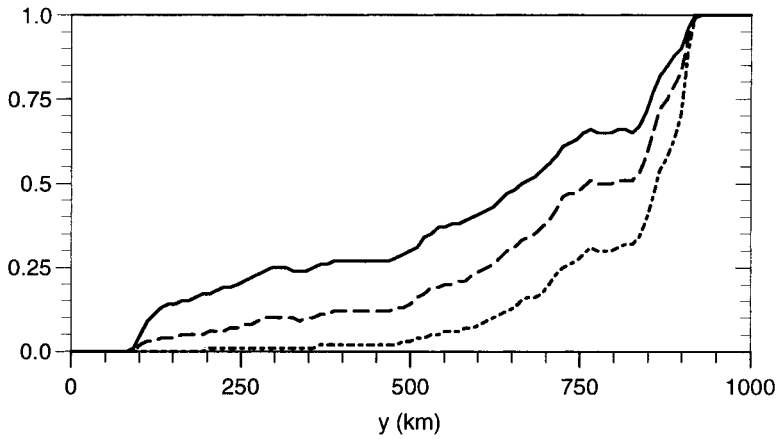

Figure 10. Meridional variations in surface tracer concentration with wind forcing after 8 years including a northern source: no surface sink (full line), tracer lifetimes of 1 year (long dashed line) or 3 months (short dashed lines).

The evolution of total nitrogen (taken as the sum of nitrate and DON) in the euphotic zone is assumed to vary as

$$\frac{D}{Dt}(\mathrm{NO_3^-} + \mathrm{DON}) = -\alpha \mathrm{NO_3^-}, \tag{8}$$

and below the euphotic zone by

$$\frac{D}{Dt}(\mathrm{NO_3^-} + \mathrm{DON}) = \frac{\partial F}{\partial z}, \tag{9}$$

where α is the rate at which nitrate is converted into particulate organic nitrogen, F is the flux of particulate organic nitrogen (defined to be positive when downward), and $D/Dt = \partial/\partial t + \mathbf{u} \cdot \nabla$ is the substantial derivative; for simplicity, we omit showing the numerical diffusion term included in (6).

The export flux of particulate organic nitrogen is given by

$$F(-h_e) = \alpha h_e \mathrm{NO_3^-}, \tag{10}$$

and the flux is assumed to decrease linearly with depth to a zero value at the base of the model, $F(z) = F(-h_e)(D + z)/(D - h_e)$; here, h_e and D are the thicknesses of the euphotic zone and water column, respectively.

The model solutions depend on the separate pathways of nitrate and DON through the system. Nitrate is also converted to DON within the euphotic zone at a rate of β, whereas DON is remineralized throughout the water column at a rate of γ. Accordingly, the DON evolution within the euphotic zone is given by

$$\frac{D}{Dt}\mathrm{DON} = \beta \mathrm{NO_3^-} - \gamma \mathrm{DON}, \tag{11}$$

and below the euphotic zone by

$$\frac{D}{Dt}\mathrm{DON} = -\gamma \mathrm{DON}. \tag{12}$$

The model is integrated either with only nitrate or both nitrate and DON included. The appropriate initial conditions and lifetimes for DON are only poorly known. The model is initialized with a total nitrogen concentration of 8 μmol N kg^{-1} over the upper four layers and 16 μmol N kg^{-1} in the bottom layer on the northern boundary. When DON is included, it has an initial condition of 4 μmol N kg^{-1} over the upper 4 layers and 0 in the bottom layer on the northern boundary. This choice for DON is broadly in accord with observed profiles in the northeast Atlantic (Doval *et al.*, 1997) and the North Pacific subtropical gyre (Hansell and Waterhouse, 1997).

Nitrate is chosen to be converted into particulate organic nitrogen at a rate, α^{-1}, of 1 week or 3 months. DON is chosen to have a longer lifetime and decay at a rate, γ^{-1}, of

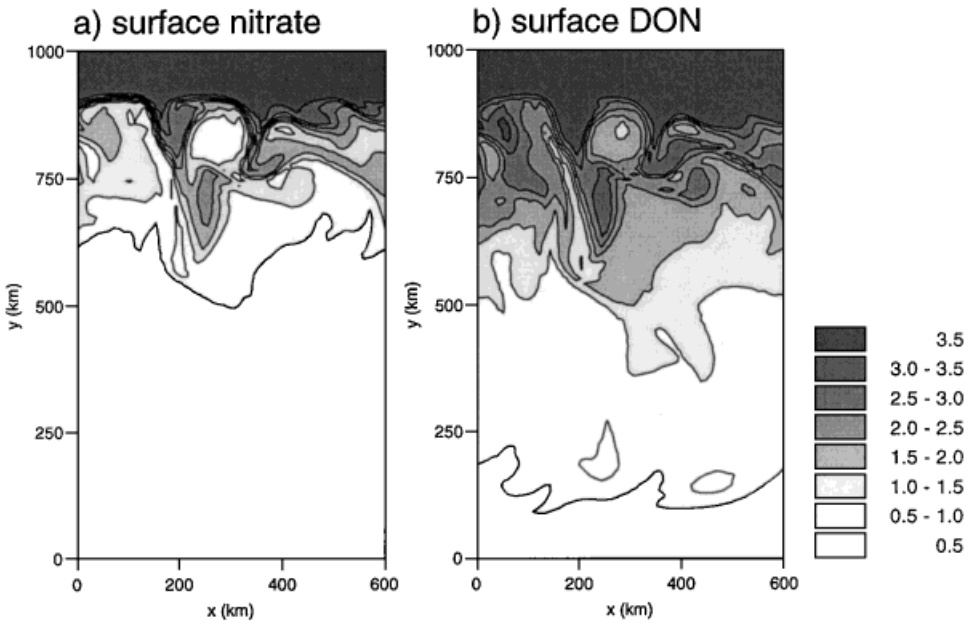

Figure 11. Maps of (a) nitrate and (b) DON concentrations (μmol N kg^{-1}) in the euphotic zone with wind forcing after 8 years including a northern source.

1 year, and be formed from nitrate at a rate, β^{-1}, of 6 months. For simplicity, the euphotic zone is assumed to have a uniform thickness h_e of 100 m, and the particulate flux is assumed to vanish at the base of the model, D, at 1000 m. The model is integrated for 8 years, when the fields become close to a statistically-steady state, with the same wind and buoyancy forcing applied as before; the overturning streamfunction is shown in Figure 8.

b. Nitrate and DON distributions

The lateral transfer of nutrients is now examined for the coupled nitrate and DON problem. Over the euphotic zone, nitrate only spreads typically 200 km equatorward from the northern source when its lifetime is 3 months (Figs. 11a and 12a). In contrast, DON spreads further into the interior, typically 400 km, when its lifetime is 1 year (Fig. 11b and 12b). Hence, this flux of DON is important in fluxing nitrogen into the euphotic zone away from the boundary zones.

The sensitivity of these results to the choice of nitrate lifetime and the presence of DON is now explored. The meridional variation in total nitrogen concentration is shown in (Fig. 13a) for different nitrate lifetimes of 1 week or 3 months. The lateral spreading is a minimum when the nitrate lifetime is only 1 week and DON is not incorporated, and increases to a maximum when the nitrate lifetime is 3 months and DON is incorporated.

The meridional flux of total nitrogen averaged over the euphotic zone, $\overline{vh}(NO_3^- + DON)/h_e$, likewise extends further into the interior whenever DON is included (Fig. 13b). This

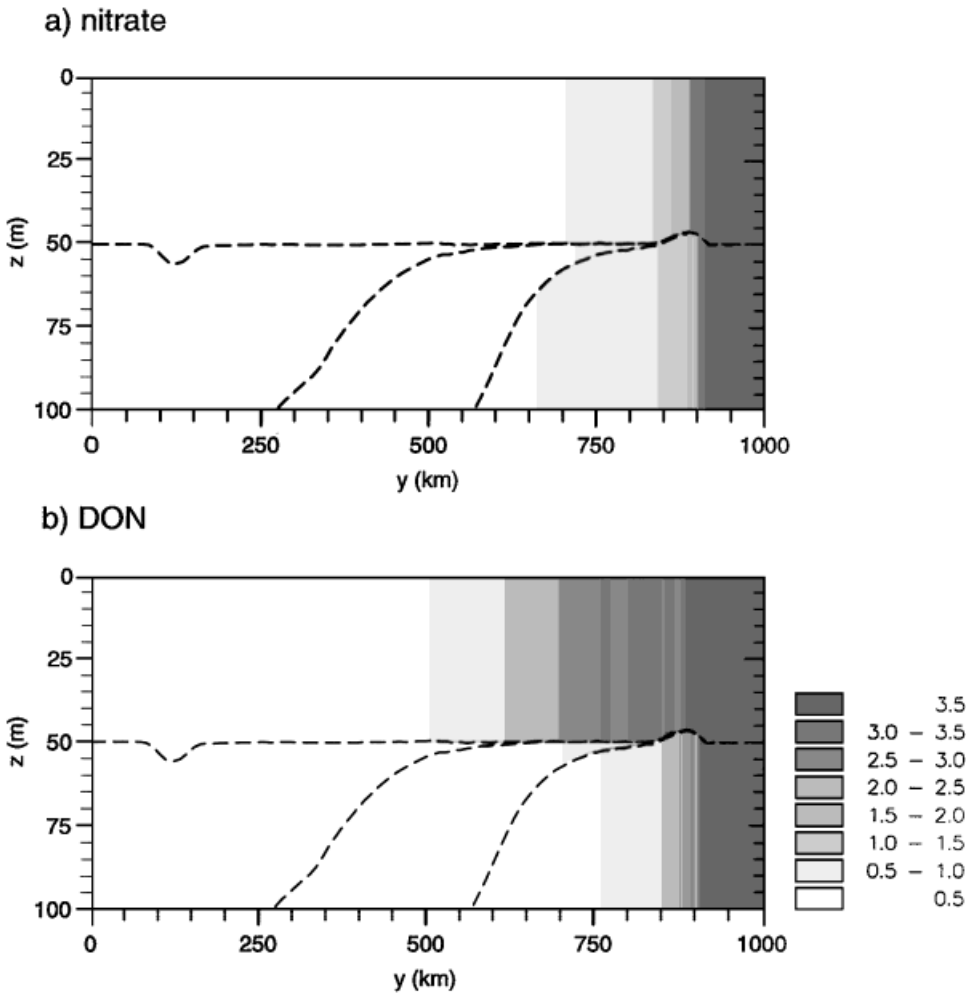

Figure 12. Meridional section for nitrate and DON over the upper 100 m with wind forcing after 8 years. A northern nutrient source is included with nitrate and DON concentrations of 4 μmol N kg^{-1} over the upper 4 layers, and a nitrate concentration of 16 μmol N kg^{-1} and no DON in the bottom layer.

nitrogen pathway involving DON is particularly important when the nitrate lifetime is short (with $\alpha^{-1} \sim 1$ week), since otherwise there is virtually no nitrogen in the euphotic zone away from the boundary source.

The export production, evaluated from the particle flux given by (10), is shown in Figure 13c. The variations in export production may be understood in terms of the steady state balance, obtained from integrating (8) over the euphotic zone and combining with (10):

$$F(-h_e) = \alpha h_e \mathrm{NO}_3^- = -\int_{-h_e}^{0} \mathbf{u} \cdot \nabla(\mathrm{NO}_3^- + \mathrm{DON})\, dz. \tag{13}$$

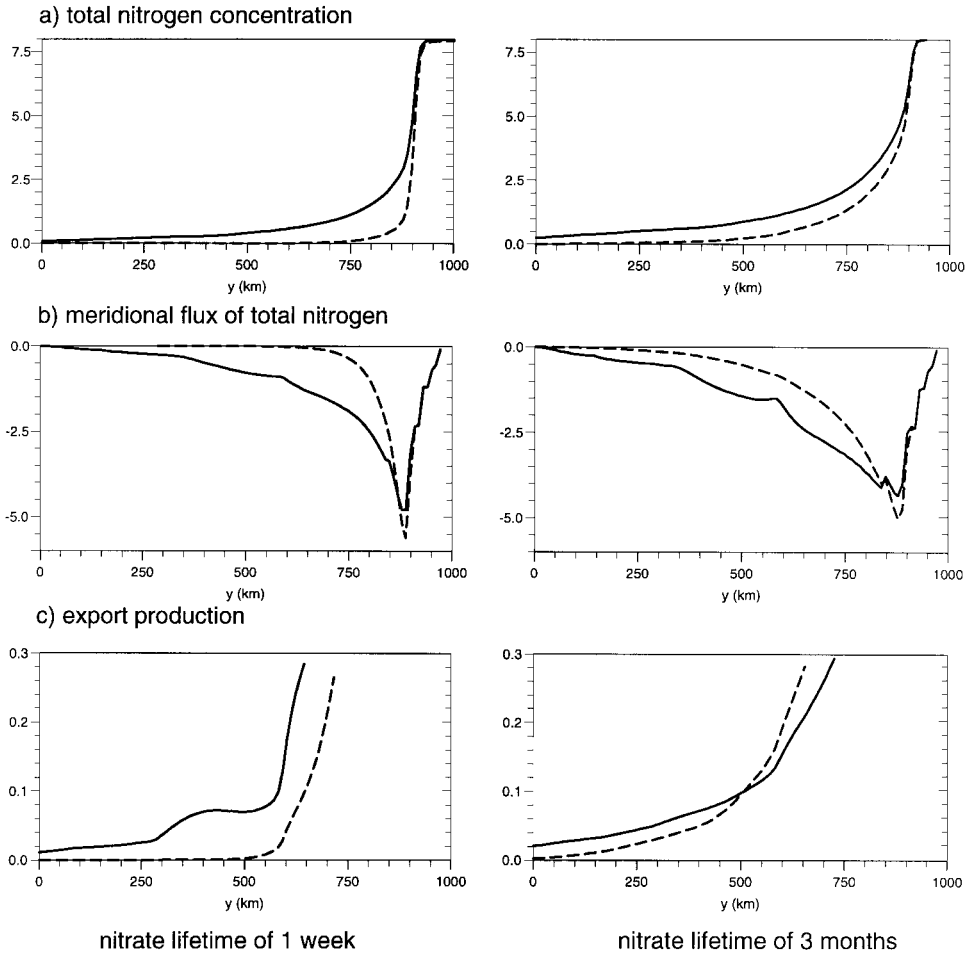

Figure 13. Meridional variations in (a) total nitrogen concentration (μmol N kg^{-1}), (b) meridional flux of total nitrogen (10^{-5} mol N m^{-2} s^{-1}) and (c) export production (mol N m^{-2} yr^{-1}) over the euphotic zone after 8 years. Cases with and without DON are shown by the full and dashed lines respectively. Case with nitrate lifetimes of 1 week and 3 months are shown by the left and right panels, respectively.

Even though export production is defined here only in terms of the consumption of nitrate, export production still depends on how the circulation transfers nitrate and DON (from the right-hand side of (13)). The export flux is generally greater in the interior when DON is included. An exception is close to the boundary, where our boundary conditions of higher nitrate for the nitrate only case gives greater export production (since we choose the total nitrogen boundary conditions to be the same in each integration). Within the model, export production is increased through DON being fluxed away from the boundary source, which

is eventually remineralised to nitrate and consumed in the euphotic zone and converted to particulate fallout.[3]

Our model estimates of export production reach the order of 0.1 mol N m^{-2} yr^{-1} over a meridional scale of several 100 km from the boundary source. In comparison, Oschlies and Garcon (1998) find a similar eddy enhancement in the nitrate input of 0.18 mol N m^{-2} yr^{-1} in the influx of nitrate to the euphotic zone (upper 126 m) over the mid-latitudes of the North Atlantic (30 to 50N) using a 1/3° resolution North Atlantic model.

Our model estimate of how far nutrients spread meridionally is sensitive to the choice of nutrient lifetime, together with the absence of seasonal cycles in the mixed layer and irradience. If seasonality is incorporated, nutrients will not be consumed during winter when there is insufficient light or beneath the euphotic zone during summer, and hence surface nutrients should spread further meridionally. This process is illustrated in a Lagrangian mixed-layer model integration for a water column passing from the subpolar gyre into the subtropical gyre, which reveals the surface nutrient signal being removed in summer, but reappearing for several winters (see Fig. 12 of Williams and Follows, 1998).

5. Discussion

The role of eddies in supplying nutrients to the euphotic zone over the sub-basin scale is examined here. On the smaller eddy and frontal scale, biological production is probably enhanced through rectified upwelling (McGillicuddy and Robinson, 1997; Mahadevan and Archer, 2000) or changes in the light biota receive through mixed-layer thickness changes (Levy *et al.*, 1998). On the larger scale, eddies provide a systematic transport and diffusion of tracers and nutrients along isopycnals. This eddy-induced transfer is crucial in controlling the spreading of tracers at depth across frontal zones and the Southern Ocean (e.g., Danabasoglu *et al.*, 1994; Marshall, 1997).[4]

For the euphotic zone, there is a competition between consumption of nutrients and the lateral transfer of nutrients through eddy-induced advection and diffusion, and time-mean advection. The eddy diffusion always acts to transfer nutrients down-gradient and is the dominant process for any short-lived tracer. The advective transport can be up- or down-gradient, and dominates for long-lived tracers. The eddy-induced advection and Ekman advection become particularly important across intergyre boundaries and frontal zones, where the time-mean geostrophic streamlines become aligned with the intergyre boundary or frontal zone. The Ekman transfer can generally supply nutrients to oligotro-

3. In reality, semi-labile DON is probably remineralized by bacteria to ammonium, which is then utilized by primary producers—in our view, this process still represents an input of 'new' nitrogen to the euphotic zone. Anderson and Williams (1999) model the cycling of organic matter and obtain DON lifetimes of 0.4 years at the surface and increasing to 6 years at 1000 m due to the lack of bacteria at depth.

4. The large-scale effects of the eddy-induced advection and diffusion might be parameterized following Gent *et al.* (1995) and Visbeck *et al.* (1997) for nutrients. Levy *et al.* (1999) has performed a recent case study parameterizing the eddy transfer associated with a convective chimney, which suggested that the large-scale effects were captured, although the estimates of biological production were sensitive to the chosen lateral diffusivity.

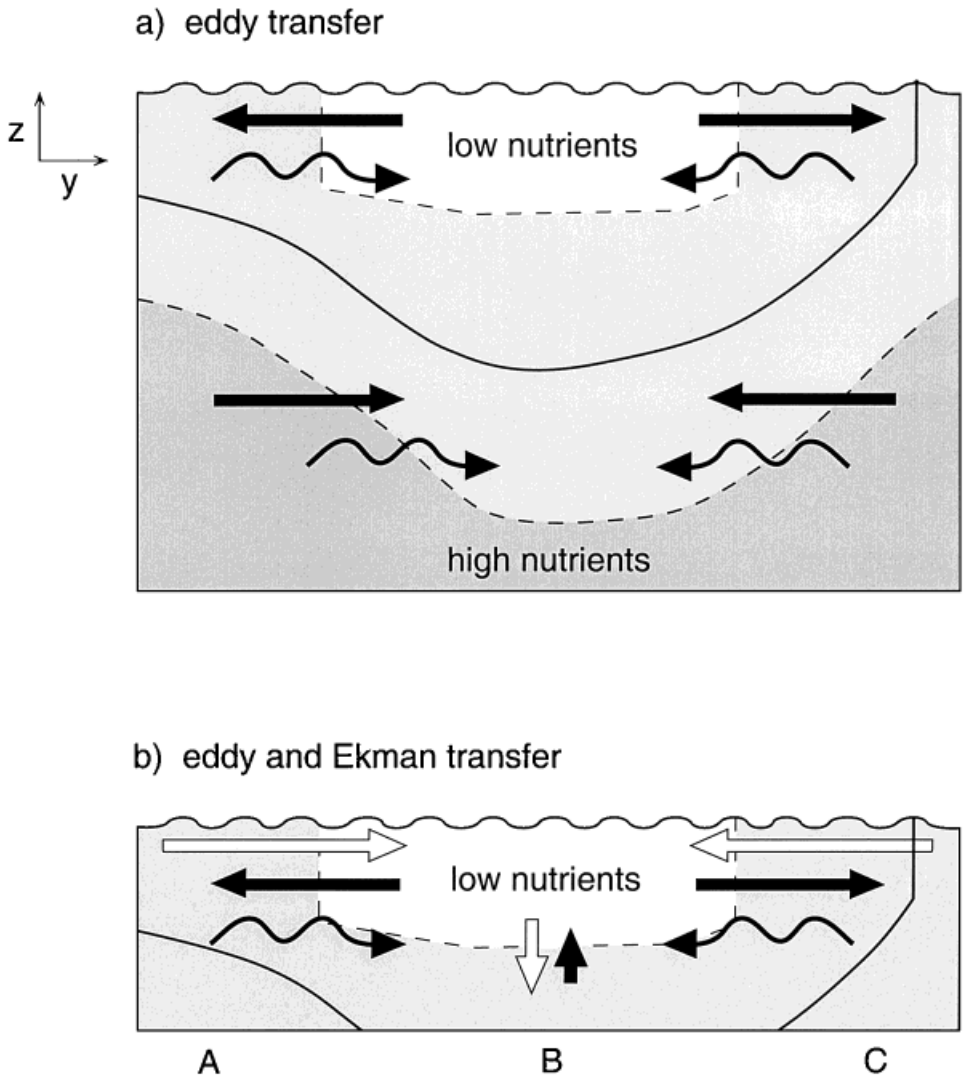

Figure 14. Schematic of the eddy-induced lateral transfer of nutrients. Section AC may be viewed as passing through a subtropical gyre or section AB as through the Southern Ocean. In (a), the eddy-induced advection (black straight arrows) and diffusion (curly arrows) oppose each other at the surface, but reinforces each other at depth. In (b), the Ekman advection (white arrow) is included, which probably dominates over the opposing, eddy-induced advection. Hence, the combination of the eddy and Ekman transfer should lead to an influx of nutrients into the interior of the subtropical gyre or a northward transfer across the Circumpolar Current.

phic surface waters through the lateral transfer from neighboring upwelling regions with high nutrient concentrations (Williams and Follows, 1998).

The eddy-induced advection attempts to flatten isopycnals and stratify the water column. The eddy advection only increases the biological production *if* the light fluid transferred into the euphotic zone is nutrient rich, which might be possible over the frontal scale, but is unlikely over the basin scale. Over the basin scale, inorganic nutrient concentrations generally increase with *density,* as revealed in gyre-scale undulations of the nutricline reflecting those of the pycnocline. Hence, the eddy-induced flattening of isopycnals over the basin scale will act to reduce the nutrient supply to the euphotic zone and *inhibit* biological production.

Over a subtropical gyre, biological production is enhanced through eddy-induced diffusion and Ekman advection supplying nutrients to the euphotic zone, but opposed by eddy-induced advection (see section AC in Fig. 14). The Ekman advection (white arrows) dominates over eddy-induced advection (black arrows). The meridional spreading of nutrients at the surface in oligotrophic waters is controlled by the nutrient lifetime and probably also by the seasonal cycle in light and mixing. At depth, the sign of the eddy-induced advection reverses and can reinforce the diffusion. This eddy-induced supply at depth might be important in offsetting the loss of nutrients in the thermocline implied through any rectified upwelling of nutrients into the euphotic zone.

For the Southern Ocean, there is an on-going debate as to the relative importance of the Ekman transfer (Toggweiler and Samuels, 1995) and the eddy-induced transport (Danabasoglu *et al.,* 1994) in controlling the meridional overturning and tracer transport. There is probably a partial cancellation between the Ekman-induced, time-mean transport and the eddy-induced transport. For the nutrient transfer, we speculate that at the surface there is a northwards transfer across the Circumpolar Current through the combined action of the northwards Ekman advection and eddy-induced diffusion, which is opposed by the southwards eddy-induced transport or 'bolus' velocity (see section AB in Fig. 14); see Marshall (2000) for a related discussion for dynamic tracers.

In summary, eddies provide a systematic, large-scale, isopycnic transfer of tracers and nutrients through a combination of diffusion and rectified advection. Whether the eddies act to enhance or inhibit biological production depends on the location of the nutrient source and the nutrient lifetime. For realistic, large-scale scenarios, the eddy-induced advection and diffusion oppose each other at the surface and reinforce each other at depth. The combination of the Ekman and eddy transfer of organic nutrients might be particularly important in maintaining biological production over the oligotrophic subtropical gyres. In particular, this surface influx of organic nutrients might offset the divergence of the nitrate flux diagnosed over the North Atlantic as proposed by Rintoul and Wunsch (1991).

Acknowledgments. MML is grateful to the Programme of Transport of the Atmosphere and Oceans for an extended visit to Trieste and support from Alessandro Crise. We are grateful for discussions with Mick Follows, Bill Jenkins, David Marshall and George Nurser.

REFERENCES

Anderson, T. R. and P. J. L. Williams. 1999. A one-dimensional model of dissolved organic carbon cycling in the water column incorporating combined biological-photochemical dependence. Global Biogeochem. Cycles, *13,* 337–349.

Archer, D., E. T. Peltzer and D. Kirchman. 1997. A timescale for cycling of DOC in equatorial Pacific surface waters. Global Biogeochem. Cycles, *11*, 435–452.

Bleck, R. and L. T. Smith. 1990. A wind-driven isopycnic coordinate model of the North and Equatorial Atlantic Ocean. 1. Model development and supporting experiments. J. Geophys. Res., *95*, 3273–3285.

Danabasoglu, G., J. C. McWilliams and P. R. Gent. 1994. The role of mesoscale tracer transports in the global ocean circulation. Science, *264,* 1123–1126.

Denman, K. L. and M. R. Abbott. 1994. Timescales of pattern evolution from cross-spectrum analysis of advanced very high resolution radiometer and coastal zone color scanner imagery. J. Geophys. Res., *99,* 7433–7442.

Doval, M. D., F. Fraga and F. F. Perez. 1997. Determination of dissolved organic nitrogen in seawater using Kjeldahl digestion after inorganic nitrogen removal. Oceanologica Acta, *20,* 713–720.

Gent, P. R., J. Willebrand, T. J. McDougall and J. C. McWilliams. 1995. Parameterizing eddy-induced tracer transports in ocean circulation models. J. Phys. Oceanogr., *25*, 463–474.

Hansell, D. A. and T. Y. Waterhouse. 1997. Controls on the distribution of organic carbon and nitrogen in the eastern Pacific Ocean. Deep-Sea Res., Part I, *44,* 843–857.

Jackson, G. A. and P. M. Williams. 1985. Importance of dissolved organic nitrogen and phosphorus to biological nutrient cycling. Deep-Sea Res., Part I, *32*, 223–235.

Lee, M.-M., D. P. Marshall and R. G. Williams. 1997. On the eddy transfer of tracers: advective or diffusive? J. Mar. Res., *55,* 483–505.

Levy, M., L. Memery and G. Madec. 1998. The onset of a bloom after deep winter convection in the northwest Mediterranean Sea: mesoscale process study with a primitive equation model. J. Mar. Sys., *16,* 7–21.

Levy, M., M. Visbeck and N. Naik. 1999. Sensitivity of primary production to different eddy parameterizations: a case study of the spring bloom development in the northwestern Mediterranean Sea. J. Mar. Res., *57,* 427–448.

Mahadevan, A. and D. Archer. 2000. Modeling the impact of fronts and mesoscale circulation on the nutrient supply and biogeochemistry of the upper ocean. J. Geophys. Res., *105,* 1209–1225.

Marshall, D. P. 1997. Subduction of water masses in an eddying ocean. J. Mar. Res., *55,* 201–222.

—— 2000. Vertical fluxes of potential vorticity and the structure of the thermocline. J. Phys. Oceanogr., *30,* 3102–3112.

McGillicuddy, D. J. and A. R. Robinson. 1997. Eddy-induced nutrient supply and new production in the Sargasso Sea. Deep-Sea Res., Part I, *44,* 1427–1449.

Najjar, R. G., J. L. Sarmiento and J. R. Toggweiler. 1992. Downward transport and fate of organic matter in the ocean: Simulations with a general circulation model. Global Biogeochem. Cycles, *6,* 45–76.

Oschlies, A. and V. Garcon. 1998. Eddy-induced enhancement of primary production in a model of the North Atlantic Ocean. Nature, *394,* 266–269.

Rhines, P. B. 1982. Basic dynamics of the large-scale geostrophic circulation. Summer Study Program in Geophysical Fluid Dynamics, Woods Hole Oceanographic Institution, 1–47.

Rintoul, S. R. and C. Wunsch. 1991. Mass, heat, oxygen and nutrient fluxes and budgets in the North Atlantic Ocean. Deep-Sea Res. Part I, *38,* S355–S377.

Strass, V. 1992. Chlorophyll patchiness caused by mesoscale upwelling at fronts. Deep-Sea Res., *39,* 75–96.

Toggweiler, J. R. and B. Samuels. 1995. Effect of Drake Passage on the global thermohaline circulation. Deep-Sea Res., Part I, *42*, 477–500.

Visbeck, M., J. Marshall, T. Haine and M. Spall. 1997. On the specification of eddy transfer coefficients in coarse resolution ocean circulation models. J. Phys. Oceanogr., *27*, 381–402.

Williams, R. G. and M. J. Follows. 1998. The Ekman transfer of nutrients and maintenance of new production over the North Atlantic. Deep-Sea Res., *45*, 461–489.

Williams, R. G., A. J. McLaren and M. J. Follows. 2000. Estimating the convective supply of nitrate and implied variability in export production over the North Atlantic. Global Biogeochem. Cycles, *14*, 1299–1313.

Yamanaka, Y. and E. Tajika. 1997. The role of dissolved organic matter in the marine biogeochemical cycle: studies using an ocean biogeochemical general circulation model. Global Biogeochem. Cycles, *11*, 599–612.

Received: *7 March, 2000;* revised: *27 July, 2000.*